

Forming Potential of Low-Density Laminates

M. Harhash, H. Palkowski

Institute of Metallurgy (IMET), Metal Forming and Processing, Clausthal University of Technology

mohamed.harhash@tu-claustahl.de, heinz.palkowski@tu-clausthal.de

A. Carradò

Institut de Physique et Chimie des Matériaux de Strasbourg, IPCMS

adele.carrado@ipcms.unistra.fr

Abstract

Metal/polymer/metal sandwich laminates show a rising rate in a variety of applications, for instance in automotive and aircraft industry. Due to the dissimilarity between the metal skin sheets and the polymer core, characterizing the forming potential of such laminates is a necessity. In this study, steel skin sheets and polypropylene-polyethylene copolymer as core sheet – called sandwich laminates - were used. They were produced in a roll bonding process using an adhesive agent.

One major research point in IMET is investigating the effect of core and skin thicknesses on the forming behavior and mechanical properties of the sandwich laminates. Forming behavior is evaluated using deep drawing in addition to determining the forming limit curves (FLC). Bonding strength is evaluated by lap shear tests. Moreover, the durability of the steel/polymer joints are evaluated under hydrothermal ageing conditions following heating/cooling regime cycles. Basically, the mechanical properties were determined using tensile testing.

The adhesion test results show good adhesion strength and a cohesive failure mode. The lap shear strength after ageing shows no remarkable deterioration. The deep drawability of the sandwich laminates depends on the thicknesses of the layers and their volume fraction. With increasing the core thickness, the limiting drawing ratio (LDR) decreases and the probability of wrinkling in the flange area and cracking is higher as well. In case of different skin thicknesses in one sandwich, the best setting condition is

to position the thinner skin in contact with the forming tool (punch) if acceptable by design.

1 Introduction

Due to the motivation of obtaining light-weight structures in addition to better thermal and acoustic isolation properties, metal/polymer/metal sandwiches can strongly contribute in this application area.

Metal/polymer/metal laminate sandwiches can be classified into:

- a) Sound-damping laminates, where a very thin core ($\sim 50 \mu\text{m}$) is sufficient. The skins thicknesses are about 0.2-2.0 mm.
- b) Low density laminates, where the thickness of the skin and core sheets are comparable for instance the core thickness ranges between 0.2 – 0.8 mm and the skin is 0.15-0.5 mm thick. Low density laminates is the case discussed in this paper. Other area of such laminates is the fiber metal laminates FML [1], where the core is reinforced with fibers.

Several sandwich structures are already in the market since at least 10 years, namely Bondal, Litecor [2], Hylite and others. Such sandwiches can provide a satisfactory or comparable forming behavior to monolithic metal sheets. Due to the inhomogeneous structure of the sandwich laminates, it is still a need of characterizing its forming behavior.

In other studies done by the authors [3,4] the effect of different core and skin thicknesses was investigated, however, in this paper the combination 0.49/0.6/0.49 is introduced. Adhesion effects, mechanical properties as well as the forming behavior of the chosen combination were investigated and are discussed.

2 Experimental work

In this study, the sandwich laminates - called SPS - were composed of a deep drawing steel grade (skin sheets), 0.49 mm thick, and a core sheet (PP-PE copolymer foil) 0.6 mm thick. The SPS was produced through the coil coating/roll-bonding process in the lab via a two-step roll-bonding using the adhesive agent Kōratec FL 201. The detailed production procedure is described and illustrated in [5]. This type of process is utilized in the production of the commercial sandwich “Bondal” [6], characterized by steel skins and a very thin core layer ($\sim 50\mu\text{m}$).

After processing, the SPS were cut and imprinted on their surfaces using electrochemical etching for the subsequent digital image analysis (DIC). The mechanical properties were characterized by tensile testing for the monomaterials (steel and polymer) and the SPS. Standard tensile specimens according to DIN 50114 were used. The tensile test was performed using a revamped UTS universal testing machine equipped with a video-extensometer unit at a constant strain rate of 0.008 s^{-1} and 80 mm gauge length. The bonding strength was evaluated by lap shear testing according to ASTM 3165. The geometry of the samples used is shown in Fig. 1. The samples were fixed in the universal testing machine UTS with a crosshead speed of 1 mm/min.

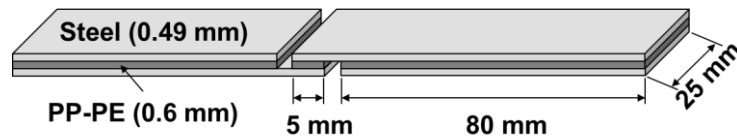


Fig. 1: Test sample for the lap shear test

The forming behavior was evaluated by deep drawing utilizing a $\varnothing 33 \text{ mm}$ flat punch and a blank of $\varnothing 68 \text{ mm}$. The drawing rate was 0.5 mm/s; the blank holding force was kept at 10 kN. The drawing procedure was performed stepwise i.e. five steps: 5, 10, 15, 20 mm and till complete drawing or failure. To estimate the susceptibility of the drawn cups to failure, the minor-major strains were compared to the forming limit curve (FLC) of the SPS.

3 Results and discussion

Fig. 2-a) illustrates the shear strength – displacement of the SPS. It can be seen that for the four test samples the deviation is about 6%. The maximum shear strength is about $11.6 \pm 0.7 \text{ MPa}$. Failure occurs within the polymer, so the failure type of the SPS is cohesive, see Fig. 2-b).

The mechanical properties in terms of the stress-strain diagram of the SPS are illustrated in Fig. 3-a). The mechanical properties of the SPS are located between those of the mono-materials. In addition to that, the strain at failure of the SPS is the same of the skin sheet, where the skin sheet in the SPS are subjected to necking and fracture first before the thermoplastic core which shows a fracture strain of 100-200%. Moreo-

ver, the properties such as yield strength (YS), tensile strength (TS) as well as the elastic modulus (E) can be compared with those estimated by the rule of mixture (ROM) as shown in Fig. 3-b). The ROM can be expressed as following:

$$\sigma_{SPS} = f \cdot \sigma_{core} + (1 - f) \cdot \sigma_{skin}, f = \frac{T_{core}}{T_{SPS}} \quad (1)$$

f is the volume fraction of the core, σ denotes the property to be calculated.

In Fig. 3-b), the estimated properties are calculated according to this rule for different f values; however the current value of SPS 0.49/0.6/0.49 is 0.38. It can be concluded that the measured mechanical has a good agreement with ROM as could be stated in [3,4].

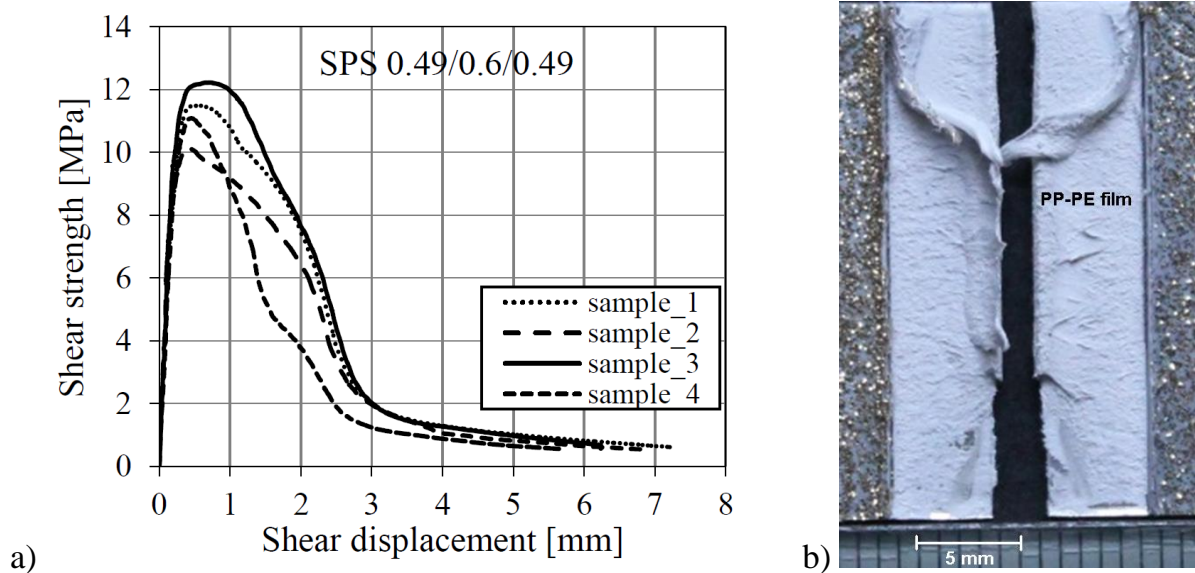


Fig. 2: a) Shear strength-displacement of the SPS and b) Failure interface.

As mentioned before, the deep drawing was performed stepwise over five steps. The forming behavior was characterized in terms of the drawing force at each step as shown in Fig. 4-a). There is a good matching between the stepwise drawing and the one step drawing. The maximum drawing load is reached at the 15 mm drawing path, decreasing further on due to the decrement of the contact/friction areas with the drawing die/blank holder. The drawing force of the monolithic steel sheet (St. 0.49 mm) is compared to that of the SPS, see Fig. 4-b). The force required to draw the SPS is double as high as that one of the steel sheet as the SPS exhibits the double thickness in steel.

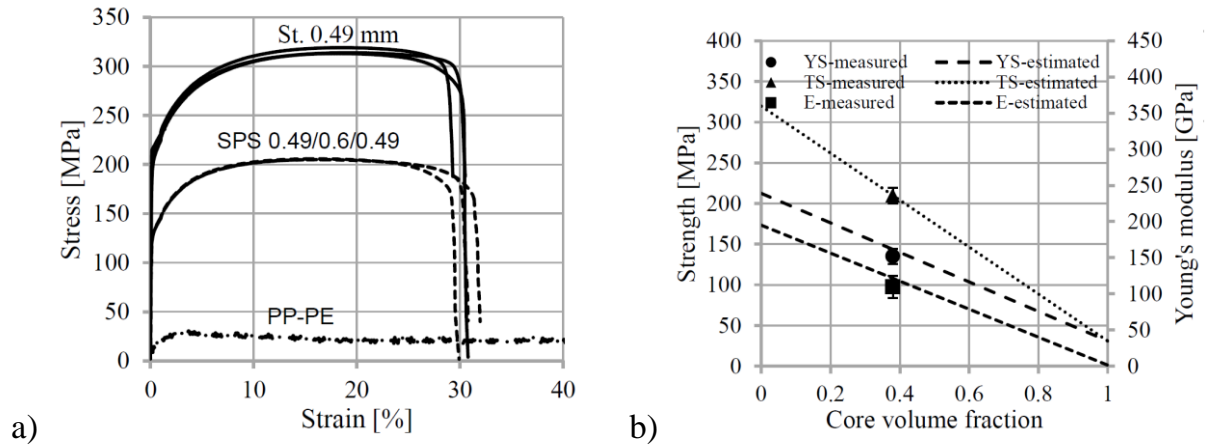


Fig. 3: a) Stress-strain diagrams of the SPS as well as the mono-materials, b) Comparison of the mechanical properties with those estimated by the rule of mixture.

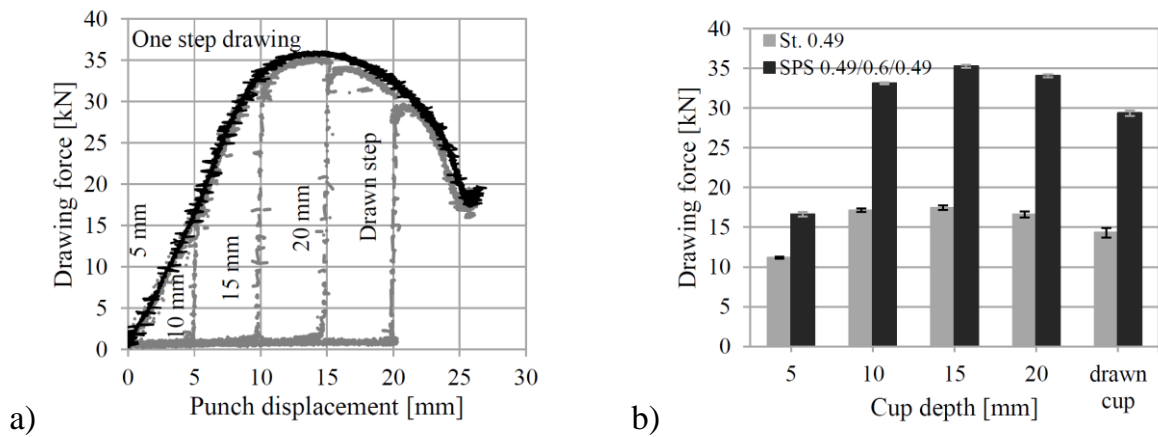


Fig. 4: a) Punch force-displacement representation in function of the five drawing steps and the single step (black), b) Comparison of the maximum drawing force at each step of the SPS 0.49/0.6/0.49 with the monolithic steel sheet (St. 049 mm).

The surface strain distribution of the steel skins were determined using the GOM-Argus system [7]. Characteristic areas of the cup are named in Fig. 5-a). The thickness reduction of the SPS as a function of the drawing depth is illustrated in Fig. 5-b). As to be expected, with increasing the cup depth, the thickness reduction increases at the punch rounding being subjected to tensile loading. The thickness reduction is estimated based on the volume consistency assumption; it is the sum of the principal strains on the surface [8]. The thickness reduction ε_3 can be expressed as $\varepsilon_3 = -(\varepsilon_1 + \varepsilon_2)$ where ε_1 and ε_2 are the major and minor strains, respectively. On the other hand, the die

rounding of the outer skin is subjected to compressive strain; consequently an increase in thickness (negative thickness reduction) is the result.

To show the tendency of the drawn cups for different drawing steps, (ϵ_1, ϵ_2) for the five steps together with the determined FLC for the SPS are demonstrated in Fig. 5-c. The FLC was determined based on time-dependent method [9,10]. It can be stated that the developed strains are far away from the FLC. Moreover, with increasing the cup depth, the minor-major strain values increase as shown in Fig. 5-c). The punch rounding is exhibiting a plane strain condition ($\epsilon_2 \approx 0$), however the die rounding is developing in compressive conditions. Moreover, the development of the strains of the cup especially at the die rounding and the punch rounding as summarized and shown in Fig. 5-d)

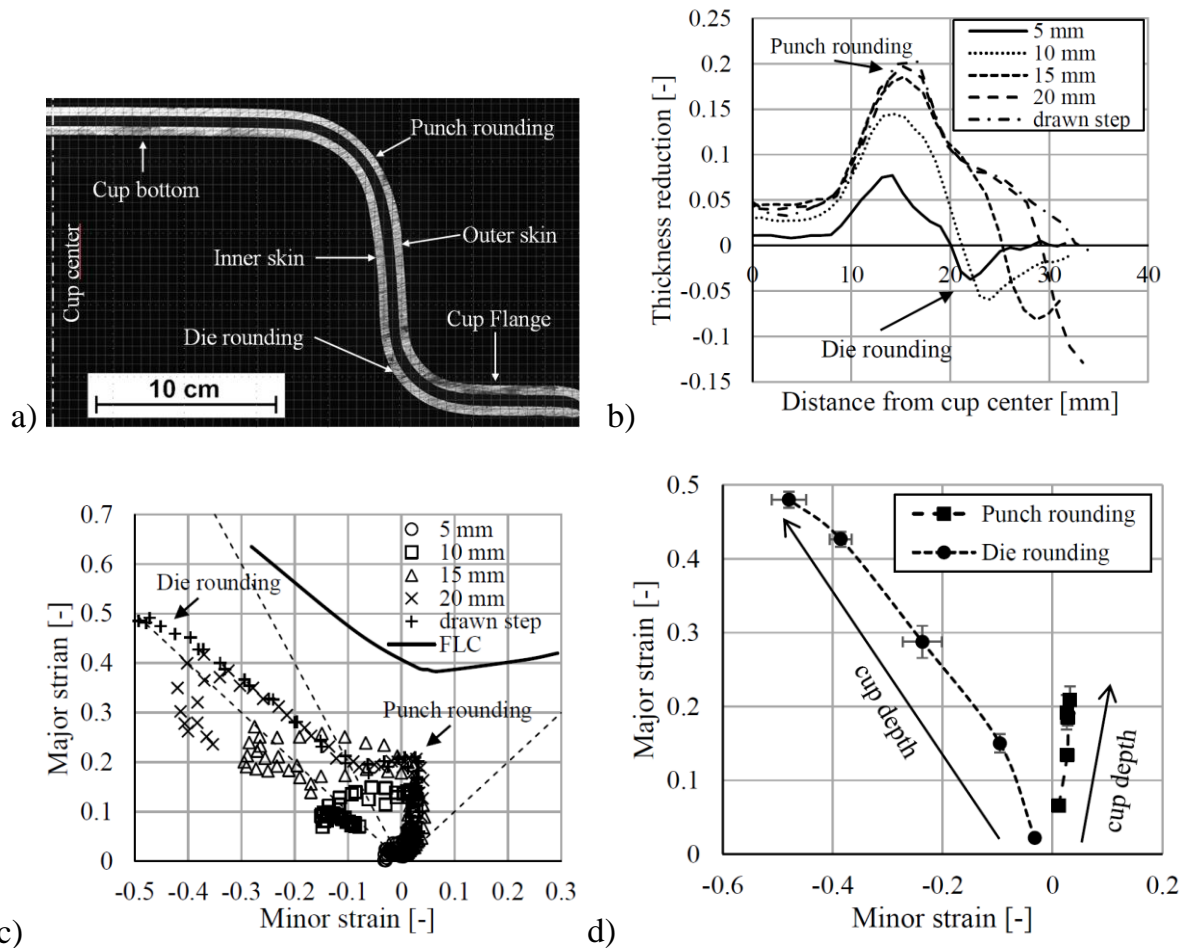


Fig. 5: a) Characteristic areas in a drawn cup, b) Thickness reduction (outer skin) in terms of the drawing depth for a radial winding off from the cup center, c) Minor-major strain distribution (outer skin) and its comparison with the FLC, d) Development of the strains at the die rounding and the punch rounding.

4 Conclusions

- The adhesion between the steel and polymer is good enough to result in a cohesive fracture after the shear test
- The mechanical properties can be estimated through the rule of mixture.
- The deep drawing behavior of the studied SPS combinations resulted in a good behavior where the strain distribution is far away from the failure limits.
- No delamination occurred under the test conditions used.
- This type of sandwich laminates exhibit extraordinary forming properties.

Acknowledgments

The authors are grateful to the German Research Foundation (DFG) as well as DAAD for the financial support.

References

- [1] Kim, J. K. and Thomson, P. F.: Forming behaviour of sheet steel laminate. *Journal of Materials Processing Technology* 22 (1990) 1, P. 45–64.
- [2] ThyssenKrupp Stahl AG: Litecor: the intelligent solution for cost-effective lightweight design, Order no. 2187 (November 2012).
- [3] Harhash, M.; Carrado, A. und Palkowski, H.: Forming Limit Diagram of Steel/Polymer/Steel Sandwich Systems for the Automotive Industry. In: *Advanced Composites for Aerospace, Marine, and Land Applications*: John Wiley & Sons, Inc. (2014), P. 243–254.
- [4] Harhash, M.; Sokolova, O.; Carradó, A. und Palkowski, H.: Mechanical properties and forming behaviour of laminated steel/polymer sandwich systems with local inlays – Part 1. *Composite Structures* 118 (2014), P. 112–120.
- [5] Sokolova, O.; Carradó, A. und Palkowski, H.: Production of Customized High-Strength Hybrid Sandwich Structures. *Advanced Materials Research* 137 (2010), P. 81–128.
- [6] ThyssenKrupp Stahl AG: Technical report: BONDAL® Composite material with structure-borne sound damping properties. (2001).
- [7] GOM: ARGUS - Optical Forming Analysis. <http://www.gom.com/metrology-systems/system-overview/argus.html>, 14.01.2015.

- [8] Marciniak, Z.; Duncan, J. L. und Hu, S. J. Ed. 2: Butterworth-Heinemann, 2002. ISBN 142948425X. Oxford, Boston.
- [9] Situ, Q.; Jain, M. K. und Metzger, D. R.: Determination of forming limit diagrams of sheet materials with a hybrid experimental–numerical approach. *International Journal of Mechanical Sciences* 53 (2011) 9, P. 707–719.
- [10] Merklein, M.; Kuppert, A. und Geiger, M.: Time dependent determination of forming limit diagrams. *CIRP Annals - Manufacturing Technology* 59 (2010) 1, P. 295–298.

Authors affiliations

Prof. Dr.-Ing. Heinz Palkowski & M.Sc. Mohamed Harhash

Technische Universität Clausthal
Institut für Metallurgie
Robert-Koch-Str. 42
38678 Clausthal-Zellerfeld, Germany

Telefon: 05323-72 2014

Telefax: 05323-72 3537

E-Mail: heinz.palkowski@tu-clausthal.de & mohamed.harhash@tu-clausthal.de

Dr. Adele Carradò

IUT Louis Pasteur, Université de Strasbourg
Institut de Physique et Chimie des Matériaux de Strasbourg
UMR 7504 UDS-CNRS, 23 rue du Loess, BP 43, 67034 Strasbourg cedex 2, France

Telefon: +33 (0)3 88 10 7105

Telefax: +33 (0)3 88 10 7248

E-Mail: adele.carrado@ipcms.unistra.fr